



Discovery of orthotolyloxyacetamides as inhibitors of NOTUM using 3D-QSAR and molecular docking studies

Reda EL-Mernissi¹, Khalil EL Khatabi¹, Ayoub Khaldan¹,
Mohammed Aziz Ajana¹, Mohammed Bouachrine^{1,2} and Tahar Lakhlifi¹

¹Molecular Chemistry and Natural Substances Laboratory. Science Faculty, Moulay Ismail University of Meknes. Morocco

²EST Khenifra. Sultan Moulay Sliman University. Benimellal. Morocco

Received 29 April 2020,
Revised 21 May 2020,
Accepted 24 May 2020

Keywords

- ✓ orthotolyloxyacetamide
- ✓ molecular Docking,
- ✓ 3D-QSAR,
- ✓ NOTUM,
- ✓ CoMFA, CoMSIA.

a.ajanamohammed@fs.umi.ac.ma
Phone: +212630345342;

Abstract

Secreted from the pineal gland, the hormone melatonin mediates several physiological effects including signaling regulation of Wnt/ β -catenin. The modification of the wnt palmitoleate lipid is important for its signaling activity while carboxylesterase Notum can extract and inactivate the lipid from wnt. Hence, notum enzyme inhibition can upregulate wnt signals. Our main objective to discover potent molecule inhibitors of Notum, suitable for exploring wnt signaling regulation in the central nervous system, there are just a few studies of combined Notum inhibitors with compounds. In this study, a series of 30 orthotolyloxyacetamides as inhibitors of Notum, were subjected to 3D-QSAR studies including CoMFA and CoMSIA, in addition, the statistical reliability is high and strong CoMFA predictability ($Q^2=0.56$, $R^2=0.91$, $r^2_{ext}=0.95$) and CoMSIA ($Q^2=0.58$, $R^2=0.97$, $r^2_{ext}=0.98$) an external test set consisting of 8 compounds was validated for the models. We proposed new compounds with highly predicted activities based on these results and contour maps provided by the CoMFA and CoMSIA. Besides, surflex-docking is performed to validate the stability of predicted molecules with the receptor PDB code: 6R8Q.

1. Introduction

The wnt signaling pathway is composed of various signal molecules, ligands and receptors such as wnt protein and β -catenin and is very conservative in evolution [1], and the wnt pathway can also change the tumor cell metabolism and thus participate in the occurrence and development of malignant tumors by changing metabolic reprogramming [2-5], wnt family members are secreted signaling proteins that play a key role in both adult stem cell biology and embryonic development [6], dysregulation of this signal is often associated with growth-related pathologies, neurodegenerative disorders, and cancer [7], and wnt protein signaling is finely balanced to ensure normal tissue development and homeostasis. This is accomplished in part by notum, an antagonist of highly stored hidden input, notum is thought to act as a phospholipase, removing glypicans from the cell surface, and related wnt proteins [8], this carboxylesterase is a crucial negative regulator for the wnt signaling pathway, through the mediation of wnt protein depalmitoleoylation [9-10].

Our target was therefore to find potent small molecule inhibitors of Notum suitable for exploring wnt signaling regulation using the Three-Dimensional Quantitative Structure-Activity Relationship (3D-QSAR) and predict their inhibitors activity using Comparative Molecular Field Analysis (CoMFA) and Comparative Molecular Similarity Indices Analysis (CoMSIA) methods [11-12], the molecular docking study was conducted using Surflex-docking method to identify essential site residues involved

in the binding modes between bioactive molecules (19, X₁, X₂, X₃) and the target protein receptor 6R8Q and indicated the reliability safety of the proposed compounds.

2. Material and Methods

A database of experimentally reported 30 orthotolyloxyacetamides as inhibitors of notum were extracted from a published study [13], database was subdivided randomly into two sets, 22 compounds were for the training set and 8 test set compounds was selected to build QSAR models. The IC₅₀ (μM) of orthotolyloxyacetamides was converted to the corresponding pIC₅₀ (pIC₅₀ = -log IC₅₀), because pIC₅₀ is more refined. Figure 1 represents the Chemical structure of the studied molecules, and Table 1 represents the different structures of compounds and their biological activities pIC₅₀ using Sybyl 2.0 software.

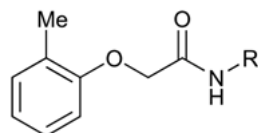


Figure 1: Chemical structure of the studied compounds.

2.1. Minimization and alignment

Molecular structures of the studied compounds were constructed and minimized using Sybyl program [14] using the Tripos standard force field [15] with Gasteiger-Hückel atomic partial charges [16] by the Powell method with a convergence criterion of 0.01 kcal/mol Å. The aim of the molecular alignment is to improve models of 3D-QSAR, the molecules were all aligned using the best active compound (compound 19) as template, utilizing the simple alignment protocol in Sybyl, Figure 2 shows the set of superimposed structures and the common nucleus.

2.2. 3D QSAR Studies

In order to determine the contributions of the steric, electrostatic, hydrophobic, H-bond donor -, and acceptor fields and to create predictive 3D QSAR models, CoMFA and CoMSIA studies based on molecular alignment methods were employed. In the literature, these studies were performed as previously descriptive [17].

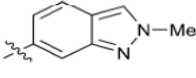
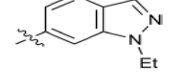
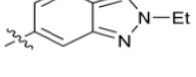
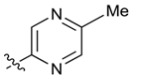
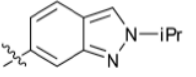
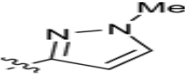
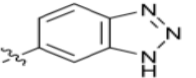
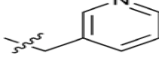
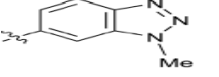
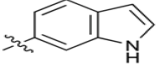
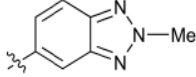
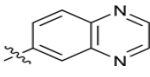
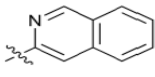
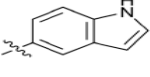
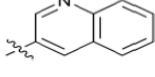
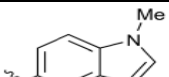
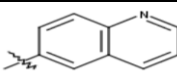
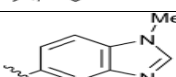
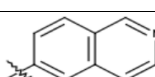
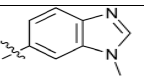
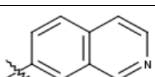
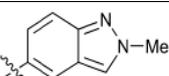
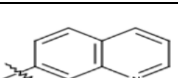
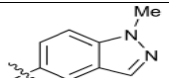
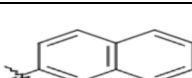
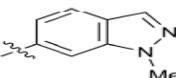
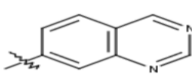
2.3 CoMFA and CoMSIA

The models CoMFA and CoMSIA have been used for to determine the several fields. The CoMFA model determined steric and electrostatic. While CoMSIA gives steric, electrostatic, hydrophobic, H-bond donor, and acceptor. The CoMFA interaction fields (steric+ electrostatic) were calculated at each grid intersection point of a regularly spaced 2.0 Å°. All the models were generated via Sybyl-X 2.0. while the charges of every structure were calculated by the Gasteiger-Hückel method.

2.4. PLS Analysis

The Partial Least Square (PLS) method in 3D-QSAR is generally performed to evaluate a linear correlation between the target variable (orthotolyloxyacetamides inhibitory activity (pIC₅₀)) and the independent variables (CoMSIA and CoMFA models) [18]. The PLS was used to determine the cross-validation coefficient Q², non-cross-validated correlation coefficient R² with a minimal number of components N and the smallest cross-validation standard error of estimate S_{ev}, the best QSAR models have been chosen based on a combination of R² and Q² values (Q² > 0.50 and R² > 0.60). The external validation of various models was confirmed using eight molecules as a test set.

Table1: Observed activities of orthotolylloxyacetamides derivatives (1-30) as inhibitors of NOTUM

<i>N</i>	R	pIC₅₀	<i>N</i>	R	pIC₅₀
1		4.481	16		6.553
2		5.796	17		6.699
3		5.027	18		7.167
4		5.444	19		7.495
5		4.143	20		6.921
6		4.000	21		6.357
7		6.678	22		6.569
8		6.167	23		5.131
9		6.481	24		5.602
10		6.620	25*		5.921
11		6.284	26*		7.071
12		6.009	27*		6.013
13*		6.444	28*		6.367
14*		6.569	29*		4.824
15		6.569	30*		6.174

* Test set molecules

2.3 Y-Randomization Test

The Y-Randomization was performed to validate the obtained models [19], the Y vector (-logIC₅₀) is shuffled at random several times, and a new QSAR model is created after each test, The new QSAR models are observable to have low Q² and R² values compared to those in the original models, a suitable

3D-QSAR model can not be produced for this data set because of structural redundancy and chance correlation.

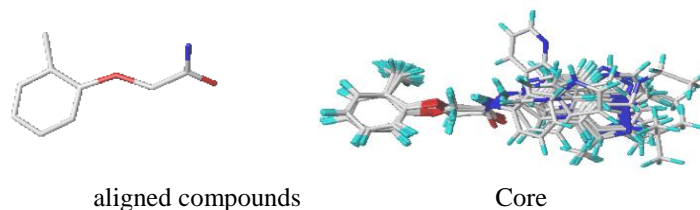


Figure 2: 3D-QSAR aligned compounds using compound 19 as a template

2.4 Molecular Docking

Confirming contour maps for COMSIA and COMFA, we are studying the binding interactions of the most active compound (19), and the proposed compound (X₁, X₂, X₃) with the enzyme (6R8Q).

The surflex-Dock [20] module of Sybyl -X 2.0 was employed for molecular docking studies, the ligands and protein preparation steps for the docking protocol were carried out in Sybyl-X 2.0 under default parameters then the results were analyzed using Discovery Studio 2016 and pymol [21] programs.

2.4.1. Macromolecule preparation

The structure of receptor (6R8Q) retrieved from the Protein Databank PDB site (www.rcsb.org) was prepared using Discovery Studio 2016 and Pymol software's.

2.4.2. Ligand preparation

The different 3D structures of the ligands (compounds 19) and proposed compounds (X₁, X₂, X₃) were constructed using Sybyl 2.0. Three-dimensional structures were minimized under the Tripos standard force field with Gasteiger-Hückel atomic partial charges by conjugated gradient method with a gradient convergence criterion of 0.01 kcal/mol Å in SYBYL software.

3. Results and discussion

3.1. CoMFA results

PLS summary shows that the CoMFA model has the cross-validated determination coefficient Q² (0.56) with three optimum numbers of components, High value for the non-cross-validated coefficient of correlation R² (0.91), F (58.10) value, and small estimation error Scv (0.32). QSAR model 's external predictive ability is usually cross-checked and validated using test sets. The external validation gave a high value of r²ext (0.95), signifying that CoMFA model predictability is acceptable. Also, the ratios of steric and electrostatic contributions were determined to be 56:44 suggesting that steric interactions are much more significant than electrostatic interactions.

3.2 CoMSIA results

The CoMSIA model result showed an acceptable value of the non-cross-validated R²=0.97 value, Cross-validated Q²=0.58, with optimum number of 4 elements, test value F=138.44, normal estimation error Scv=0.18, and very high external validity value r²ext=0.98. The proportions of steric, electrostatic, hydrophobic, H-bond donor, and H-bond acceptor contributions accounted for 10%, 22%, 19%, 28%, and 21%, respectively. Table 2 results obtained showed that both the CoMFA and CoMSIA models were reasonable and reliable for predicting inhibitor activities. Table 3 displays the experimental and predicted pIC₅₀ of the training and test sets. Figure 3 indicates a strong linear association between the measured pIC₅₀ values and those observed.

Table 2: Statistical results of the CoMFA and CoMSIA models

Model	Q ²	R ²	S _{cv}	F	N	r ² _{ext}	FRACTION				
							Ster	Elec	Hyd	Don	Acc
CoMFA	0.56	0.91	0.32	58.10	3	0.95	0.56	0.44	-	-	-
CoMSIA	0.58	0.97	0.18	138.44	4	0.98	0.10	0.22	0.19	0.28	0.21

Q²: Cross-validated correlation coefficient; R²: Non-cross-validated correlation coefficient; N: Optimum number of components; S_{cv}: Standard error of the estimate; r²_{ext}: External validation correlation coefficient; F: F-test

Table 3: inhibitors and predicted activities of orthotolyloxyacetamides.

N ^o	pIC ₅₀	CoMFA		CoMSIA	
		Predicted pIC ₅₀	Residuals	Predicted pIC ₅₀	Residuals
1	4.481	4.439	0.042	4.387	0.094
2	5.796	5.885	-0.089	5.853	-0.057
3	5.027	5.102	-0.075	5.088	-0.061
4	5.444	5.071	0.373	5.052	0.392
5	4.143	4.119	0.024	4.094	0.049
6	4.000	3.907	0.093	4.112	-0.112
7	6.678	6.853	-0.175	6.830	-0.152
8	6.167	6.154	0.013	6.140	0.027
9	6.481	6.305	0.176	6.288	0.193
10	6.620	6.442	0.178	6.435	0.185
11	6.284	6.466	-0.182	6.443	-0.159
12	6.009	6.002	0.007	6.027	-0.018
13*	6.444	6.070	0.374	6.228	0.216
14*	6.569	6.386	0.183	6.335	0.234
15	6.569	6.463	0.106	6.445	0.124
16	6.553	6.513	0.040	6.519	0.034
17	6.699	6.611	0.088	6.617	0.082
18	7.167	7.120	0.047	7.246	-0.079
19	7.495	7.208	0.287	7.259	0.236
20	6.921	6.655	0.266	6.710	0.211
21	6.357	6.548	-0.191	6.598	-0.241
22	6.569	6.462	0.107	6.516	0.053
23	5.131	5.253	-0.122	5.269	-0.138
24	5.602	5.438	0.164	5.375	0.227
25*	5.921	6.289	-0.368	6.346	-0.425
26*	7.071	6.683	0.388	6.676	0.395
27*	6.013	6.050	-0.037	6.063	-0.050
28*	6.367	5.907	0.460	5.921	0.446
29*	4.824	5.465	-0.641	5.520	-0.696
30*	6.174	5.829	0.345	5.789	0.385

* Test set molecules

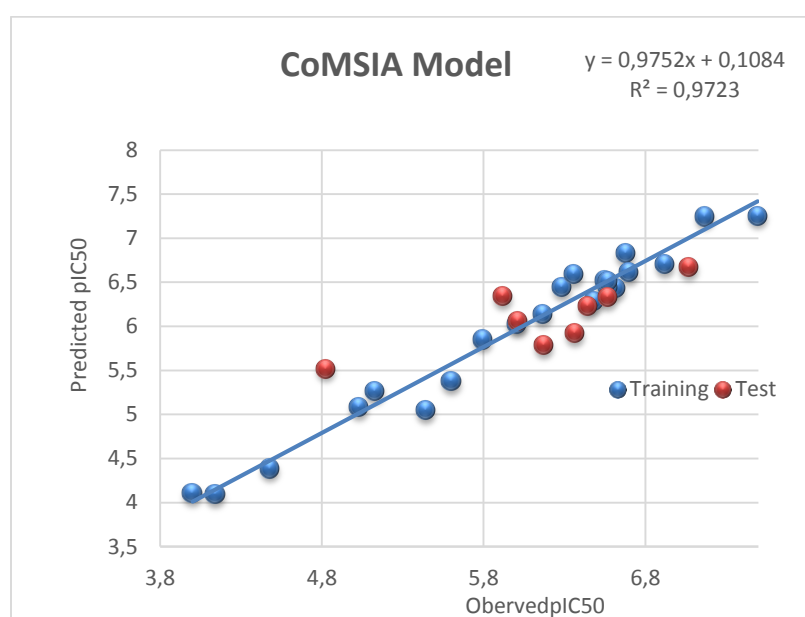
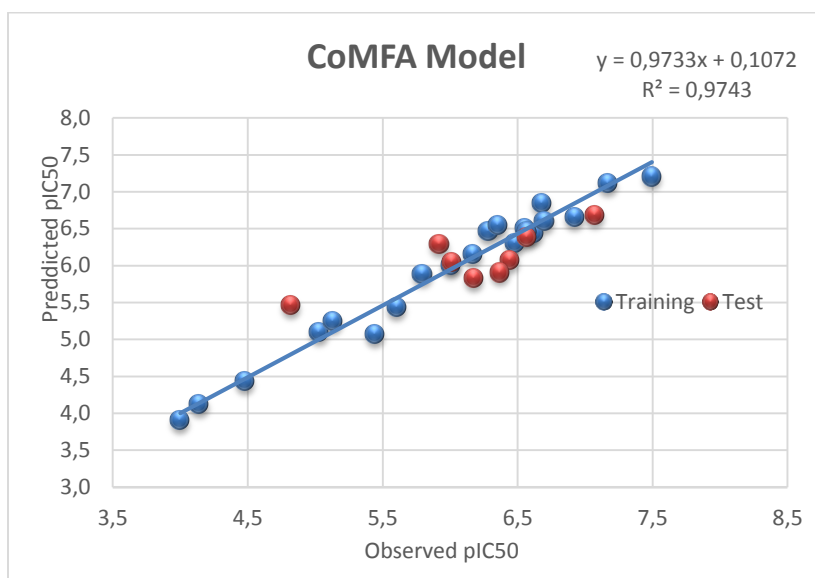


Figure3: Experimental versus predicted activity of the training and test set based on the CoMFA and CoMSIA model.

We note a normal distribution of activity values depending on the experimental values according to Fig 3. Also, CoMSIA Model's has of determination coefficient R^2 , F , Q^2 , and r^2_{ext} are greater than that of CoMFA, while Scv is lower.

3.3 Graphical Interpretation of CoMFA and CoMSIA

We have renamed each substituent of the most active molecule 19 to facilitate the description of the contours, Fig 4 displays newly developed chemical structure. CoMFA and CoMSIA contour maps were produced to streamline regions where the activity can be increased or decreased. CoMFA contours are displayed in Figure 5 (a, b), while CoMSIA contours are illustrated in Figure 6 (a, b, c). In the Analysis, compound 19 was used as a reference structure.

3.3.1 CoMFA Contour Maps

The contour maps of CoMFA steric field are presented with yellow (20% contribution) and green (80% contribution) colors while electrostatic interactions are presented with blue (80% contribution) and red (20% contribution) colored contours.

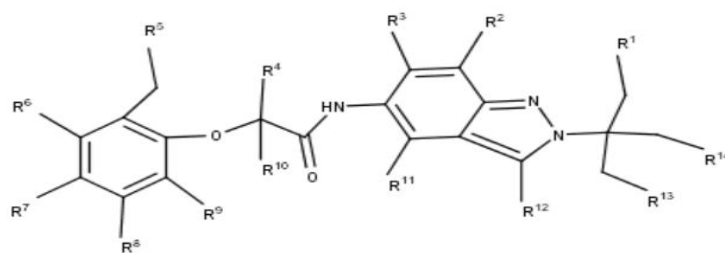


Figure 4: chemical structure of newly design

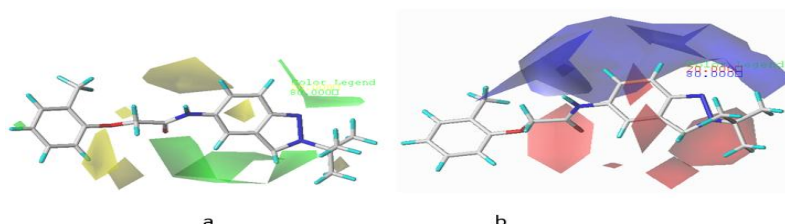


Figure 5: CoMFA contour maps with compound 19 as template. **(a)** Steric: Green contours favored bulky regions, and yellow contours bulky disfavored regions. **(b)** Electrostatic: field shown in (bleu) indicates favored region and (red) indicate disfavored region.

In the CoMFA steric contour map [Fig \(5a\)](#): Yellow contours around the substituents R^9 and R^3 , this color suggested that adding a large substitution in this region would be disadvantageous to the activity.

While the green contours is seen near of the substituents R^{11} , R^{12} , R^{13} and the NH groups which is adjacent to the (C=O) group on the one hand, and between the substituents R^1 and R^2 , which suggests that inhibitors with bulky groups at these positions could increase the inhibitory activity.

In the [Fig \(5b\)](#): the blue contours select all the substituents between R^1 and R^4 , indicating that electron-donating substituents are favored in these positions which would exhibit good activity. But the red contours select except the substituents R^{10} and R^{13} , the position indicates that the addition of an electronegative substituent may help to increase inhibitory activity in this position.

3.3.2 CoMSIA Contour Maps

In the CoMSIA we used the electrostatic, H-bond donor, and H-bond acceptor fields because they have a higher percentage compared to other fields, these fields are represented in [Fig 6 \(a, b, c\)](#) with compound 19 as the template molecule. The same structure of compound 19 used in CoMSIA to facilitate interpretation, we also used in CoMFA.

In the CoMSIA electrostatic contour map [Fig \(6a\)](#): The blue contours select all the substituents R^4 , NH and R^3 positions, suggesting that electron-donating groups would increase the activity and the red contours select except the substituents R^2 and R^{12} can decrease the activity.

The hydrogen-bond donor field was presented in [fig \(6b\)](#): The purple contour turns around substituents between R^1 and R^5 , except for R^3 selected by cyan contour, the purple contour revealed that hydrogen bond donor was not preferred in this region, which indicated that adding substituents type the hydrogen-bond acceptor might increase the activity. Magenta contour [fig \(6c\)](#) can be seen around substituents R^1 , R^{13} , R^{12} and R^{10} , which informs that hydrogen bond acceptor substituent character, will increase activity, and red contour about R^{11} showed that hydrogen acceptors in this region were not preferred.

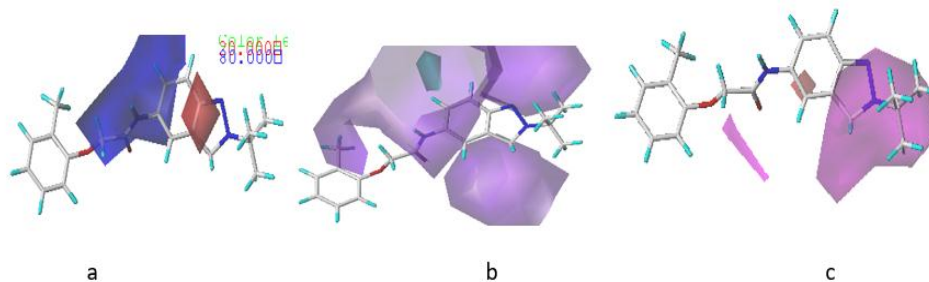


Figure 6: CoMSIA contour maps with compound 19 as template. (a) Electrostatic: Red contours indicates electron-withdrawing groups favored, and blue contours means electron-donating groups favored. (b) H-bond donor: Cyan and purple contours stand for favorable and unfavorable respectively. (c) H-bond acceptor: Magenta and red contours indicate H-bond acceptor favorable and unfavorable respectively.

3.2. Y-Randomization

The Y-Randomization method is executed to affirm the CoMSIA and CoMFA models. Diverse random shuffles of the dependent variable were performed then a 3D-QSAR was built after each shuffle the weak Q^2 and R^2 values showed that the good result in our original CoMFA and CoMSIA models is not due to a chance correlation of the training set, and the results obtained are presented in Table 4.

Table 4: Q^2 and R^2 values after random Y-randomization tests

Iteration	CoMFA		CoMSIA	
	Q^2	R^2	Q^2	R^2
1	-0.328	-0.456	-0.269	0.330
2	-0.165	0.284	0.276	-0.281
3	0.091	0.112	0.132	0.284
4	-0.230	0.271	-0.273	-0.178
5	0.243	0.405	0.302	0.312
6	0.165	0.286	0.191	0.243
7	-0.345	0.445	-0.292	0.386
8	-0.325	-0.390	-0.289	0.311
9	0.376	-0.243	0.119	0.245
10	-0.226	0.132	0.203	-0.109
11	0.232	0.247	0.314	0.211

3.4. Newly designed compounds

The six new orthotolxyacetamides derivatives (Table 5) were designed based on the 3D-QSAR (CoMFA / CoMSIA) models, the new predicted X_1 structure shows greater activity ($pIC_{50} = 7.947$ for CoMSIA) than compound 19 which is the series' most active compound (figure 7).

Table 5: Predicted pIC_{50} of newly designed molecules based on CoMSIA and CoMFA 3D- QSAR models.

N°	Predicted pIC_{50}	
	CoMFA	CoMSIA
X_1	7.590	7.957
X_2	7.564	7.962
X_3	7.561	7.932
X_4	7.549	7.891
X_5	7.512	7.881
X_6	7.506	7.872

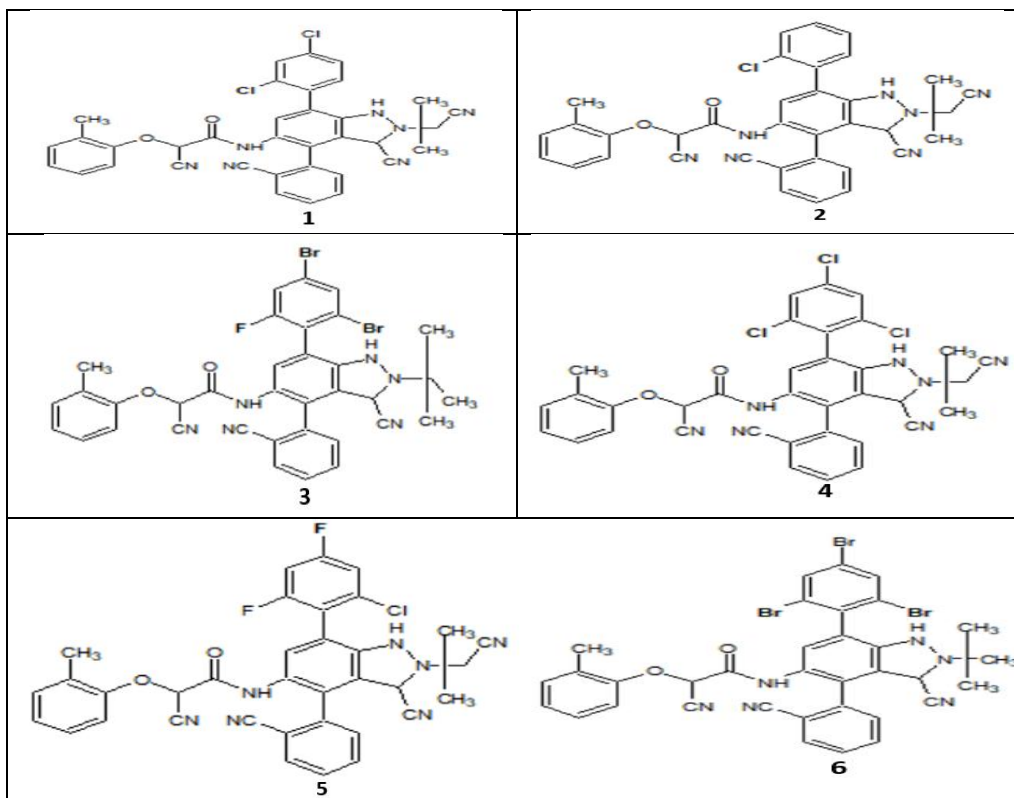


Figure 7: Structures of newly designed molecules.

3.5. Docking results

Surflex-dock was used to expound the activity of the compounds, and its relationship with the interactions between the enzyme (PDB ID: 6R8Q) and the active molecule (compound 19), the proposed molecules (X₁, X₂, and X₃).

Figure 8 shows the active compound (compound 19) presents a van der waals interaction with TRP A:128 residues, conventional Hydrogen Bond with SER A:232 residue, carbon Hydrogen Bond interaction with HIS A:389 residue, pi-sulfur interaction with MET A:143 residue, amide-pi stacked interaction with GLY A:127, alkyl and pi-alkyl interaction with ALA A: 342, ALA A: 232, ILE A:291, TYR A: 129, PHE A:319 ,PHEA:320,VAL A: 187,PHE A:268 residues. While the proposed (compound X₁) presents a carbon Hydrogen bond interaction with GLY A:127 residue, Halogen (Cl, Br, I) interaction with ALA A:342 residue, pi-anion interaction with GLUA:125 residue, pi-sigma interaction with ILE A:393 residues, pi-pi stacked interaction with TRP A: 128 residues, alkyl and pi-alkyl interaction with VAL A: 346, HIS A:389, PHE A: 123 residues.

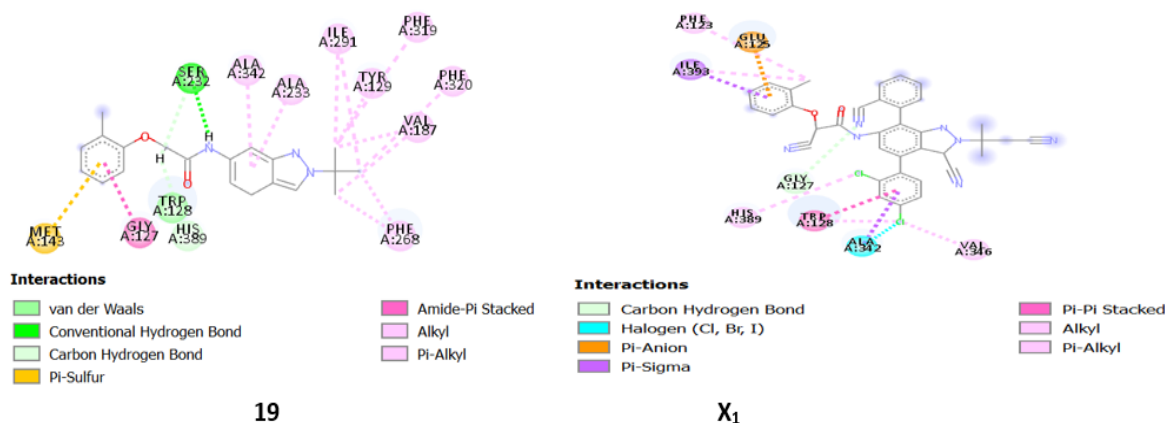


Figure 8: Docking interactions between the compounds (19, X₁) and the protein 6R8Q.

In addition, the proposed X₂ compound [figure 9](#) presents a conventional hydrogen bond interaction with ALA A:233 residues, carbon hydrogen bond interaction with THR A: 345 residues, pi-anion interaction with GLU A:390 residues, pi-donor hydrogen bond interaction with ALA A:342 residues, pi-sigma interaction with TRP A: 128 residues, pi-pi stacked interaction with HIS A:389 residues, alkyl interaction with VAL A:346. While the proposed (compound X₃) shows a conventional hydrogen bond interaction with a SER A: 232, THR A:345 residues, pi-sigma interaction with GLY A: 127 residue, pi-lone pair interaction with TRP A:128 residue, pi-pi stacked interaction with PHE A:268 residue, alkyl and pi-alkyl interaction with VAL:346, ALA A:342, HIS A:350 residue, these interactions explain the stability and the high activity of the proposed compound.

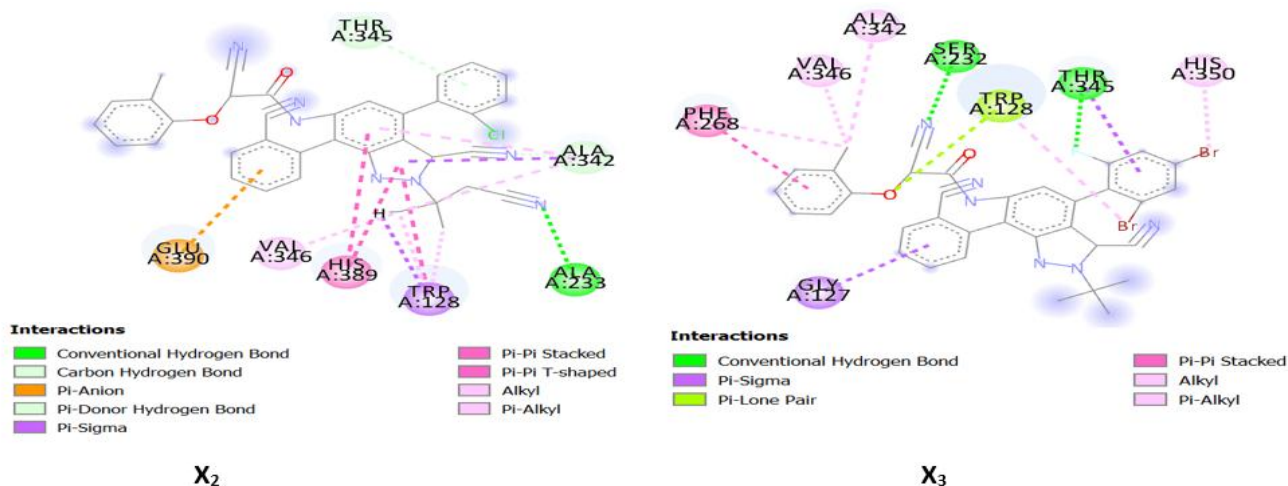


Figure 9: Docking interactions between the proposed compounds (X₂, X₃) and the protein 6R8Q.

Conclusion

In this study, 3D-QSAR Methods (CoMSIA, CoMFA) applied to 30 compounds of orthotoloxacetamides derivatives showed excellent results the CoMSIA ($R^2 = 0.97, Q^2 = 0.58$) and CoMFA ($R^2 = 0.91, Q^2 = 0.56$). Models, equally fine, had a clear understanding of the structure–activity relationship and binding modes of this series as potent inhibitors of the notum, while the molecular docking results confirmed each substituent's effect on the activity and revealed some crucial interaction between the ligands and the protein. Accordingly, six new notum inhibitors were developed, and improved inhibition activity was demonstrated.

Acknowledgements Great thanks to the “Association Marocaine des Chimistes Théoriciens” (AMCT) for its relevant help concerning the programs.

References

1. S.Y. Lee, H.M Jeon, Ju MK, et al, Wnt/Snail signaling regulates cytochrome C oxidase and glucose metabolism, *Cancer Res*, 72(14) (2012) 3607-3617.
2. P. Rada, A. Rojo, A. Offergeld, et al, WNT-3A regulates an Axin1/NRF2 complex that regulates antioxidant metabolism in hepatocytes, *Antioxid Redox Signal*, 22(7) (2015) 555-571.
3. V. Sherwood, WNT signaling: an emerging mediator of cancer cell metabolism, *Mol Cell Biol*, 35(1) (2015) 2-10.
4. H. Tao, JJ. Yang, KH. Shi, J.Li, Wnt signaling pathway in cardiac fibrosis: New insights and directions, *Metabolism*, 65(2) (2016) 30-40.

5. Adebayo Michael AO, Ko S, Tao J, et al, Inhibiting Glutamine-Dependent mTORC1 Activation Ameliorates Liver Cancers Driven by beta-Catenin Mutations, *Cell Metab*, 29(5) (2019) 1135-1150.
6. R. Nusse, H. Clevers, Wnt/ β -Catenin Signaling. Disease. and Emerging Therapeutic Modalities, *Cell*, 169(2017) 985–999.
7. P. Polakis, Wnt signaling in cancer, *Cold Spring Harbor Perspect Biol*, 4 (2012) a008052.
8. O. Gerlitz, K. Basler, Wingful, an extracellular feedback inhibitor of Wingless, *Genes Dev*, 16 (2002) 1055–1059.
9. S. Kakugawa, et al, NOTUM deacylates Wnt proteins to suppress signaling activity, *Nature*, 519 (2015) 187–192.
10. X. Zhang, et al, NOTUM is required for neural and head induction via Wnt diacylation. oxidation. and inactivation, *Dev. Cell*, 32 (2015) 719–730.
11. G. Klebe, U. Abraham, T. Mietzner, Molecular similarity indices in a comparative analysis (CoMSIA) of drug molecules to correlate and predict their biological activity, *J. Med. Chem*, 37 (1994) 4130-4146.
12. RD. Cramer, DE. Patterson, JD. Bunce, Comparative molecular field analysis (CoMFA): 1. Effect of shape on binding of steroids to carrier proteins, *J. Am. Chem. Soc*, 110(18) (1988) 5959-5967.
13. Benjamin N. Atkinson, David Steadman, Yuguang Zhao, James Siphthorp, Luca Vecchia. Reinis R. Ruza, Fiona Jeganathan, Georgie Lines, Sarah Frew, Amy Monaghan, Svend Kjær, Magda Bictash. E. Yvonne Jones and Paul V. Fish, “Discovery of 2-phenoxyacetamides as inhibitors of the Wnt-depalmitoleating enzyme NOTUM from an X-ray fragment screen, *Med. Chem. Commun*, 10 (2019) 1361–1369.
14. A. Khaldan, K. El khatabi, R. El-mernissi, A. Sbai, M. Bouachrine, T. Lakhliifi, Combined 3D-QSAR Modeling and Molecular Docking Study on metronidazole-triazole-styryl hybrids as antiamoebic activity, *Moroccan Journal of Chemistry*, 8 (1) (2020) 527-539.
15. M. Clark. R. D Cramer III and N. Van. Opdenbosch, Validation of the general purpose tripos 5.2 force field, *J. Comput. Chem*, 10(8) (1989) 982–1012.
16. William P. Purcell, Judith A. singer. A brief review and table of semiempirical parameters used in the Hueckel molecular orbital method, *J. Chem. Eng. Data*, 12(2) (1967) 235–246.
17. K. Yao , P. Liu , H. Liu , Q. Wei, J. Yang, P. Cao, Y. Lai , 3D-QSAR, molecular docking and molecular dynamics simulations study of 3-pyrimidin-4-yl-oxazolidin-2-one derivatives to explore the structure requirements of mutant IDH1 inhibitors, *Journal of Molecular Structure* 1189 (2019) 187-202.
18. S. Wold. Validation of QSAR's, *Quant. Struct. Act. Rela*, 10 (1991) 191-193.
19. X. Li, H. Zhou, X. Mo, L. Zhang, J. Li, In silico study of febuxostat analogs as inhibitors of xanthine oxidoreductase: A combined 3D-QSAR and molecular docking study, *Journal of Molecular Structure*, 1181 (2019) 428-435.
20. Sybyl 8.1; Tripos Inc.: St. Louis, MO, USA, 2008; Available online: <http://www.tripos.com> (accessed on 26 January 2011)
21. W. L. DeLano, The PyMOL molecular graphics system, [Http://Pymol. Org. \(2002\)](Http://Pymol. Org. (2002))

(2020) ; <http://www.jmaterenvirosci.com>